Available online at www.sciencedirect.com
SCIENCE @ DIRECT®

Journal of the European Ceramic Society 24 (2004) 2553–2566
www.elsevier.com/locate/jeurceramsoc

Dielectric and electromechanical properties of sol-gel prepared PZT thin films on metallic substrates

S. Seifert[a], D. Sporn[a], T. Hauke[b], G. Müller[a], H. Beige[b,*]

[a]Fraunhofer-Institut für Silicatforschung ISC, D-97082 Würzburg, Germany
[b]Martin-Luther-Universität Halle-Wittenberg, FB Physik, D-06108 Halle, Germany

Received 1 October 2002; received in revised form 21 July 2003; accepted 3 August 2003

Abstract

This article reports about the dielectric and electromechanical properties of sol-gel derived ferroelectric PZT films on metallic substrates. PZT(53/47) films deposited directly on metallic substrates (Hastelloy C-276) show a strong thickness dependence of their dielectric and electromechanical properties as well. This dependence can be described by a model assuming an interface layer between substrate and PZT film. By applying an additional electrode between substrate and PZT film the formation of the interface layer can be minimized and a significant reduction of the thickness dependence as well as a general improvement of the film properties was observed. By varying the Zr/Ti-ratio it was found that the extrema of the dielectric and piezoelectric coefficients are shifted towards Ti-rich stoichiometries compared to bulk ceramics. For PZT thin films with optimized preparation conditions nearly rectangular hysteresis loops with a coercive field strength of 5 V/μm, a piezoelectric coefficient d_{33} of 96 pm/V and strains up to 0.4% were obtained. Antiferroelectric PZT (98/2) films could be deposited in a good quality on an oxidic electrode, too. The observed field-induced antiferroelectric–ferroelectric phase transition is accompanied by high strains. Furthermore, bending resonance modes of samples with different geometries and the tip displacement of a simple cantilever under a dc-field were investigated. By controlled bending of the substrate charges up to 0.3 μC/cm^2 could be obtained. On the other hand, tip displacements of up to 30 μm could be realized by applying a voltage of 17 V/μm, respectively.
© 2003 Elsevier Ltd. All rights reserved.

Keywords: Actuators; Dielectric properties; Films; Piezoelectric properties; PZT; Sensors

1. Introduction

For ferroelectric ceramics there exists a wide range of applications due to their excellent dielectric, electromechanical, electrooptical and pyroelectric properties. The solid solution system $Pb(Zr_xTi_{1-x})O_3$ is—up to now—the mostly used material for electromechanical sensors and actuators due to the high dielectric and piezoelectric coefficients for compositions close to the morphotropic phase transition between rhombohedral and tetragonal phase at a Zr/Ti-ratio of 53/47.[1–3]

During the last decades, research on ferroelectric thin and thick films, their preparation, characterization, and application was continuously growing. Besides the application for different kinds of memories like FeRAMs or highly integrated DRAMs, the demand for microelectromechanical systems (MEMS) is one of the driving forces for the further development of ferroelectric thin film technology.[4,5]

Due to the good integrability into existing processing technologies, platinized silicon wafers are commonly used as substrates. However, other materials like thin ceramic membranes or metallic foils attract also interest.[6–9] Although a number of preparation routes like Sol-Gel processing or Pulsed Laser Deposition allow to deposit ferroelectric thin films of good quality, the properties of ferroelectric thin films are often worse than those of the stoichiometrically corresponding bulk materials.[7] Besides the small thickness and the clamping of the films by the substrate, the deposition technique and parameters as well as possible interactions between film and substrate/electrode are discussed as the main reasons for the lower property profiles of PZT thin films compared with bulk materials.[7]

* Corresponding author.
E-mail address: beige@physik.uni-halle.de (H. Beige).

0955-2219/$ - see front matter © 2003 Elsevier Ltd. All rights reserved.
doi:10.1016/j.jeurceramsoc.2003.08.007

In this paper, we report about the properties of sol-gel derived ferroelectric PZT thin films on metallic substrates of type Hastelloy C-276. This particular alloy was selected as substrate because of its high thermal and chemical stability. Special attention was paid to the piezoelectric properties with respect to various electromechanical applications. After a short description of the preparation and characterization methods, the dielectric and electromechanical properties and their correlation with preparation conditions are shown. The thickness dependence of the properties and their dependence on different electrodes are presented and discussed. Afterwards the influence of stoichiometric variations is described and discussed. Using the results gained up to here, films with optimized properties were produced and their properties important for MEMS applications like resonance modes were characterized again.

2. Basic film preparation and measurement equipment

2.1. Film and electrode preparation

The PZT thin films were prepared with a modified sol-gel process, the preparation of the deposition solution was described elsewhere.[10] Metallic foils of Hastelloy C-276 with thicknesses between 50 and 200 μm were used as substrates. If not mentioned otherwise, no additional ground electrode was used. After preannealing the substrates at 600 °C for a few minutes, the sol was deposited by a dip coating procedure, yielding single layer film thicknesses of about 0.8 μm after a thermal treatment at 600 °C for 10 min. By multiple coatings, overall film thicknesses of up to 6 μm were realized. For the preparation of ceramic bottom electrodes in the system ULSM (*U*nderstoichiometric *L*anthanum *S*trontium *M*anganate) a comparable procedure was applied.[11] For the preparation of metallic bottom electrodes, Pt was sputtered onto the substrates.

2.2. Measurement equipment

For measurements of the electrically induced longitudinal strain and the piezoelectric coefficient d_{33}, the equipment shown in Fig. 1 was used. It is based on a capacitive detector: the samples were placed between two rods, one of them freely moveable. The other side of this rod carries one plate of an air capacitor, which is a component of a HF-resonance circuit. A change of the sample thickness causes a change of the capacitance of the capacitor and thus a frequency modulation of the HF-resonance circuit. Finally, this frequency modulation is transformed into a voltage proportional to the strain of the sample by means of a modulation analyzer. A quartz connected mechanically in series with the sample is used for calibration and for accurate measurements of d_{33} by means of a compensation technique. Additionally, the polarization of the samples could be determined by a Sawyer-Tower circuit.

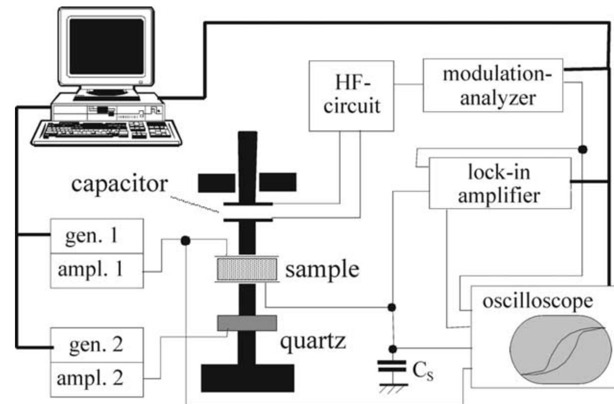

Fig. 1. Equipment for measurements of the electromechanical properties.

For the determination of the piezoelectric coefficient d_{33} the films were poled by applying an electric field for a few seconds. The field strength was chosen to be about 45 V/μm, which is at least two times the coercive field strength. The measurements of d_{33} were carried out some minutes after poling.

3. Results and discussion

3.1. Thickness dependence of the dielectric and electromechanical properties

A series of PZT (53/47) films with thicknesses varying from 0.8 to 5 μm was produced by multiple coatings. The samples were 2 cm×2 cm in size, the substrate thickness was 200 μm. On top of the samples circular gold electrodes with diameters of 1 mm were sputtered.

3.1.1. Small signal properties

Fig. 2 shows the reciprocal capacitance and the piezoelectric coefficient d_{33} versus the film thickness. For a linear dielectric material one expects that the reciprocal capacitance is proportional to the film thickness. Indeed, for the investigated films a linear dependence was observed. However, a significant offset in the 1/C-axis was found: the linear regression for zero film thickness gives a value significantly higher than zero. Such a behavior is usually explained by the existence of undesired layers at the interface(s) between the electrode(s) and the PZT-film, whose dielectric permittivities are lower than that of the ferroelectric film.[16,17,18] In the following, these layers are considered as only one layer, which is denoted as interface layer. If the thickness of this interface layer is much smaller than that of the film, a dependence

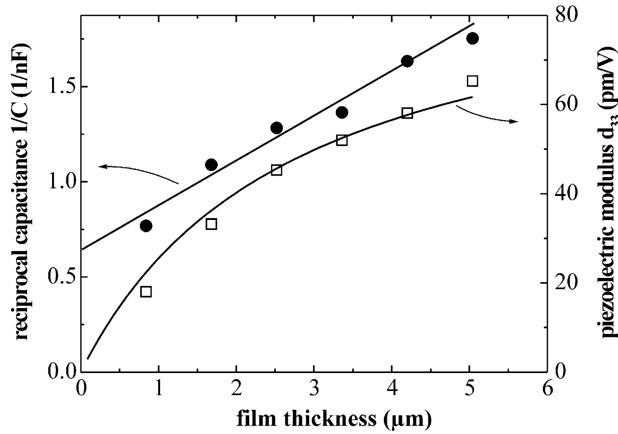

Fig. 2. Reciprocal capacitance (dot area 0.79 mm^2) and piezoelectric constant d_{33} of PZT (53/47) films on Hastelloy substrates as a function of film thickness; the lines are fits to the model explained in the text.

$$\frac{1}{C_{\mathrm{meas}}} = \frac{1}{C_{\mathrm{Interface}}} + \frac{1}{\varepsilon_0 \varepsilon_{\mathrm{film}} A} t_{\mathrm{film}} \tag{1}$$

is expected, where C_{meas} and $C_{\mathrm{Interface}}$ are the measured capacitance and the (unknown) capacitance of the interface layer, respectively. $\varepsilon_{\mathrm{film}}$ is the dielectric permittivity of the undisturbed, pure PZT-film, t_{film} the film thickness and A is the electrode area, respectively. Fitting Eq. 1 to the experimental data provides a capacitance of $C_{\mathrm{Interface}} = (1.5 \pm 0.2)$ nF for the interface layer and a dielectric permittivity of the undisturbed PZT-film of $\varepsilon_{33} = 610 \pm 120$. This value for ε_{33} is about 60% of the typical value reported for bulk ceramics with a comparable stoichiometry.[12]

The piezoelectric coefficient d_{33} behaves similar to the dielectric permittivity: As shown in Fig. 2, d_{33} increases strongly with increasing film thickness. For a film thickness of approximately 5 μm typical d_{33}-values of 60 pm/V were found. Again, the observed thickness dependence can be ascribed to the existence of an interface layer. Using the same assumptions as for Eq. (1) and neglecting a possible piezoelectric behavior of the interface layer, the thickness dependence of the piezoelectric coefficient d_{33} can be expressed by

$$d_{33,\mathrm{meas}} = \frac{d_{33,\mathrm{film}}}{1 + \frac{\varepsilon_0 \varepsilon_{\mathrm{film}} A}{C_{\mathrm{Interface}} t_{\mathrm{film}}}}, \tag{2}$$

where $d_{33,\mathrm{meas}}$ is the measured piezoelectric coefficient and $d_{33,\mathrm{film}}$ is the piezoelectric coefficient of the undisturbed film, respectively. The fit of Eq. (2) by taking only $d_{33,\mathrm{film}}$ as a unknown constant describes the data rather well, and a piezoelectric coefficient $d_{33,\mathrm{film}}$ of 95 pm/V can be obtained. Again, this value is lower than those reported for bulk ceramics with typical d_{33} values of about 270 pm/V.[12]

There are many possible explanations for these observations, like local variations in the film stoichiometry or microstructural inhomogenities, like pores and inclusions. Amongst all others, the mechanical clamping of the films by the substrate has to be taken into account.

The piezoelectric induced lateral strain of the film is suppressed due to the mechanical connection of the film with the stiff substrate with a significantly higher thermal expansion coefficient.[14,15] For typical substrate materials, like SiO_2 or Al_2O_3, and for typical ratios between film and substrate thickness higher than 1:10, the suppression is nearly perfect.[13] This clamping results in a reduction of the effectively measurable piezoelectric coefficient d_{33} to approximately 50% of the value for a free ceramics.[13]

Using this value, the piezoelectric coefficient of a hypothetically free standing PZT film on Hastelloy would be about 190 pm/V. This corrected value is closer to the values of bulk ceramics, nevertheless it is still about 70% of the typical value of bulk ceramics.

A further reason for the lowered piezoelectric coefficient of the films on Hastelloy compared to bulk ceramics is thought to be due to the observed typical microstructure of the samples. As one can see in the TEM-micrographs of Fig. 3, the films exhibit a closed porosity with pores of about 50–200 nm in size. The pores are distributed homogeneously throughout the whole film; only a small region near the interface seems to be dense. The observed porosity might play a role in the electromechanical interactions of the ferroelectric grains with the surrounding microstructure. Furthermore, the porosity may lead to a lack of stable domain configurations in the grains, i.e. most grains are single domain. Indeed, no domain walls could be observed by TEM-investigations and therefore, extrinsic contributions might be absent, too. As a consequence, this would lower d_{33} and ϵ_{33} as compared with bulk ceramics.

3.1.2. Large signal dielectric and electromechanical properties

Fig. 4 shows typical dielectric and electromechanical hysteresis loops for samples with different film thickness. The loops are symmetrical with respect to the electric field; with increasing film thickness the hysteresis loops get more pronounced. The coercive field strength decreases from 20 V/μm for a 0.8 μm thick film to about 9.5 V/μm for a 5 μm thick film. Simultaneously, the remanent and maximum polarization increase to maximum values of about 40–50 μC/cm^2. For the butterfly loops, the maximum strain increases and the hysteresis becomes smaller with increasing film thickness, whereas the remanent strain of $S_{\mathrm{rem}} \approx 0.085\%$ is nearly thickness independent.

Fig. 3. Typical TEM micrograph of a PZT(53/47) film on Hastelloy substrate. In the micrograph the upper layer of a 5-fold sample is shown. The film exhibits closed porosity (bright dots) throughout the whole film thickness. Only the surface of each layer seems to be dense.

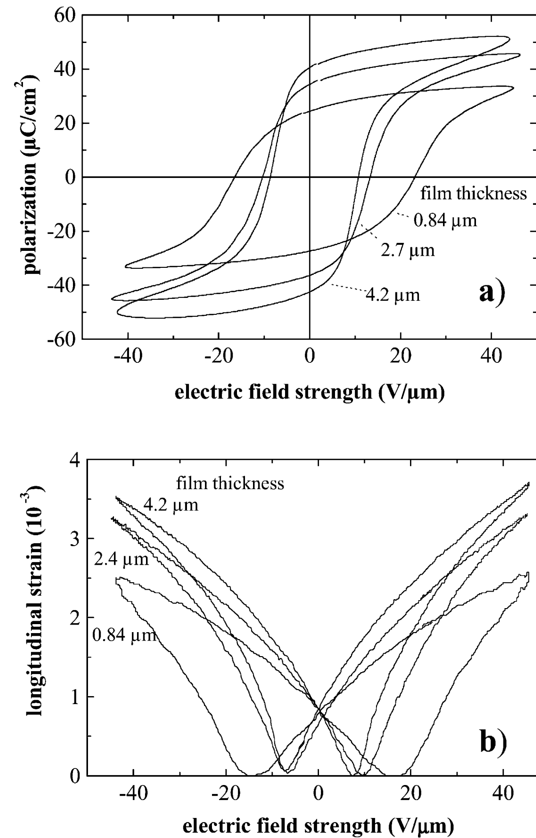

Fig. 4. Dielectric and electromechanical hysteresis loops for three different film thicknesses.

Fig. 5 shows the coercive field strength as a function of the film thickness. Again it can be seen, that the coercive field strength decreases continuously with increasing film thickness. Some authors explain such a dependence with the existence of a pure *dielectric* (i.e. non ferroelectric) interface layer,[16–18] as we mentioned in Section 3.1.1, too. However, other authors point out, that for such a system the coercive field strength should be independent of the film thickness,[19] which would be in contrast to the observations.

For the calculations of these models a number of different, hardly to measure parameters have to be taken into account, for example thickness and permittivity of the interface layer, or remanent polarization and coercive field strength of the pure film. Therefore, we have used another model for a description of the thickness dependence of the coercivity E_C. The PZT film (totally N single layers) is thought to consist of two regions, the first PZT layer at the substrate on one hand, and the remaining N-1 layers on the other hand. The interface layer and the first PZT layer are put together for the model, or in other words, the interface layer is seen as a part of the first PZT-layer. This point of view has two advantages.

First, the macroscopic properties of this ‘‘unit’’ can be measured directly; no additional assumptions or estimations concerning parameters of the interface layer are necessary. As a consequence the second advantage is, that it is not necessary to distinguish, whether the interface layer itself is ferroelectric or a pure dielectric. Moreover, origin and nature of the interface layer do not play any role in this model. However, from the comparison between model and experimental data no additional information about the pure interface layer can be extracted.

With these assumptions, the hysteresis loop of the whole PZT film can be seen as a ‘‘series connection’’ of the hysteresis loop of the first PZT layer and that of the remaining N-1 layers. The calculation of the resulting hysteresis loop of such a system is still difficult. For simplifying the problem some simplifications were made:

- (i) It is assumed, that all PZT layers have hysteresis loops with a strictly rectangular shape.
- (ii) The hysteresis loops of both components differ only in their coercive field strengths, i.e. the remanent polarisation is the same for all layers, which is schematically shown in Fig. 6.

With these assumptions, the resulting hysteresis loop is again of rectangular shape and the coercive field strength can be calculated from

$$E_{\mathrm{C,meas}}\ t_{\mathrm{film}} = \sum_{\forall i} E_{C,i} t_i, \tag{3}$$

where $E_{\mathrm{C,meas}}$ and t_{film} denote measured coercive field strength and thickness of the whole film, respectively. The subscript i denotes the corresponding properties of the ith layer. In our model we have to distinguish only between the first layer with a coercive field strength E_{C1} directly determinable from experimental data, and the other N-1 layers consisting of "pure" PZT with coercivity $E_{\mathrm{C,PZT}}$. Than, the coercive field strength of the whole film is finally given by

$$E_{\mathrm{C,meas}} = E_{\mathrm{C,PZT}} + \frac{t_1}{t_{\mathrm{film}}}\left(E_{\mathrm{C,1}} - E_{\mathrm{C,PZT}}\right). \tag{4}$$

The only unknown parameter in Eq. (4) is $E_{\mathrm{C,PZT}}$, which can easily be determined from fitting Eq. (4) to the experimental data (Fig. 5). Despite the simplifications, especially the assumed constant remanent polarization for all layers, a quite good agreement between measured data and fit is observed, and a coercive field strength of the pure film of $E_{\mathrm{C,PZT}=}7.1$ V/μm can be obtained.

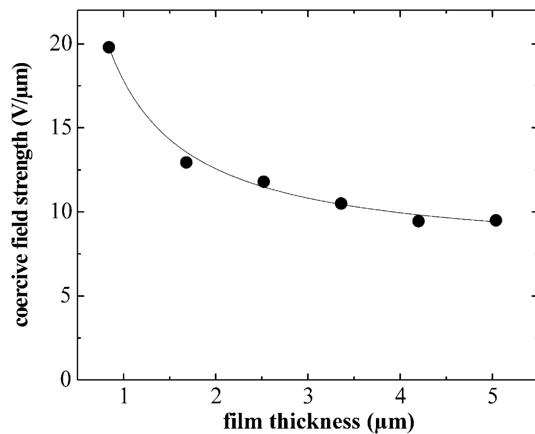

Fig. 5. Dependence of the coercive field strength on the film thickness; the lines correspond to a fit according to Eq. 4.

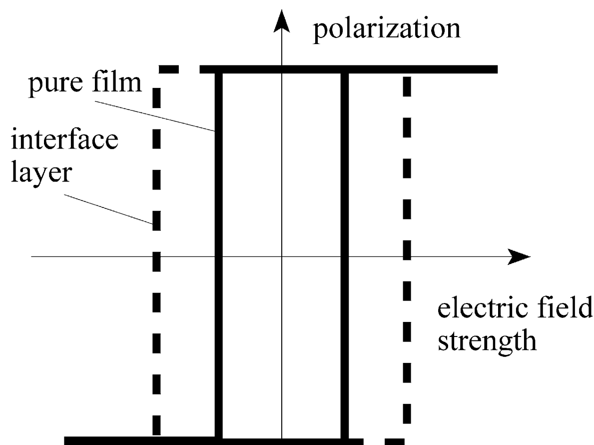

Fig. 6. Schematic illustration of the hysteresis loops of a pure PZT film and an interface layer assumed for the modeling of the thickness dependence.

3.1.3. Investigations of the interface

For a better understanding of the observed thickness dependence, the samples were investigated by means of XRD, SEM and TEM. Neither in the XRD nor in the SEM any further information about possible reasons for the observed thickness dependence were obtained. By using a plan-view preparation technique described elsewhere[20] a sample with electrontransparent regions could be obtained and investigated. Besides some morphological effects, like an enhanced porosity and amorphous regions, TEM-EDX measurements of this sample across the interface between substrate and film indicate significant variations of the elements Pb, Zr, and Ti of PZT as well as Ni and Cr from the Hastelloy substrate. The measurements shown in Fig. 7 were carried out in steps of 50 nm. As one can see, the Cr is relatively high at the film side of the interface, followed by an increase of the Ni content more inside the PZT film. The Pb content at the interface is relatively high, too. Obviously, there exists a secondary phase at the interface, containing Pb and Cr that could be identified to $PbCrO_5$.[20] Additionally, the Ni-diffusion into the PZT seems to act as a hard-doping of the PZT and deteriorates the physical properties.[21]

As a consequence the existence of an interface layer, which is formed between substrate and film, can be seen as one main reason for the observed strong thickness dependence of the properties, as could be shown by one model. Nevertheless, the electromechanical and dielectric properties of the hypothetically undisturbed PZT films derived from the model are still inferior to those of corresponding bulk ceramics.

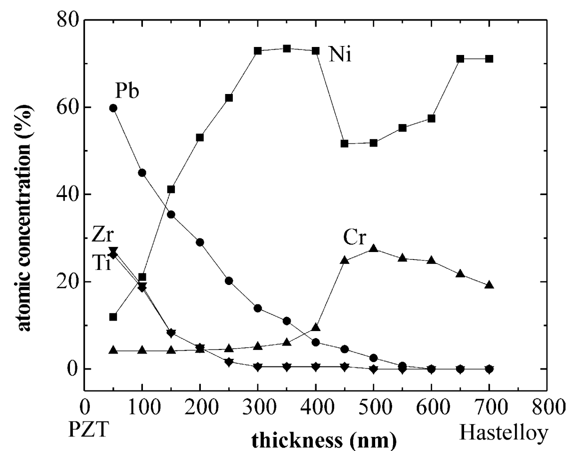

Fig. 7. EDX-scan across the interface in plan-view mode. The scan steps are 50 nm.

3.2. Control of the interface

As a consequence of these results, a film optimization with respect to the interface is expected to lead to improved film properties. For this reason, different methods for controlling the interface have been tested. Preannealing the Hastelloy substrates to achieve a controlled oxidic NiO-layer on the surface failed, the deposited PZT films were of worse quality than without annealing. It is well known that the material of the electrodes can strongly influence the properties of the films.[22,23] In order to check whether this holds also valid for the PZT-films on Hastelloy, several attempts for controlling the substrate–film interface by using additional substrate electrodes were made.

3.2.1. Variations of the substrate electrode

Two different types of substrate electrodes have been tested, Platinum as a metallic electrode and oxidic electrodes within the system ULSM. The platinum layer was sputtered onto the Hastelloy foils.[1] The oxidic ULSM electrode was prepared from a precursor solution on the metallic substrate by a spin-coating process. The typical electrical resistivity of these oxidic electrodes was determined by the van-der-Pauw method to be of about 10 Ω cm.[24] For comparison, investigations of films on the unelectroded Hastelloy substrate are shown here again. All PZT samples were prepared by a four-cycle spin-coating process, resulting in a final overall film thickness of about 0.8 μm. Gold electrodes were sputtered as top electrodes and the properties of the films were investigated.

Fig. 8 shows the typical dielectric and electromechanical hysteresis loops of the three samples. For both types of additional substrate electrodes remarkable improvements of the film properties were observed: the coercive field strength is about 8 V/μm for films on Pt and ULSM compared with 20 V/μm for films deposited directly onto the substrate. Remanent and maximum polarization are also remarkably higher in the case of additional electrodes. In the electromechanical hysteresis loops remarkably higher strains are observed and the hysteresis is much less pronounced. Characteristic values of the large signal behavior are shown together with the small signal behavior in Table 1.

An improvement of the film properties is observed in the small signal behavior, too. Both, the dielectric permittivity ϵ_{33} and the piezoelectric coefficient d_{33} are much higher for films on Pt and on ULSM compared to films without additional bottom electrode, as can be seen from Table 1.

In the electromechanical behavior nearly no differences between films on Pt and ULSM can be seen (Fig. 8, Table 1). In the dielectric behavior, the coercive field strength is nearly the same for both types of additional substrate electrodes, whereas the remanent polarization and the dielectric permittivity for films on ULSM are somewhat higher than those of films on Pt.

These results indicate that the formation of an interface layer between the Hastelloy substrate and the PZT-film can be efficiently suppressed by applying a sandwiched substrate electrode. The type of electrode has only a minor influence on the resulting film properties. However, the obtained values for d_{33} and ϵ_{33} for example, are still smaller than the corresponding values for bulk materials. Moreover, they are somewhat smaller than the values obtained for much thicker PZT films prepared directly on the substrate (see Section 3.1). Therefore it is argued that the formation of the interface layer

Table 1
Characteristic average properties of PZT(53/47) films for different types of bottom electrodes

PZT-films on electrode	E_C (V/μm)	S_{max} (10^{-3})	$\varepsilon_{33}/\varepsilon_0$	d_{33} (pm/V)
None (pure Hastelloy)	21	1.9	185	13
ULSM-electroded Hastelloy	8.2	3.1	790	47
Pt-electroded Hastelloy	7.3	3	610	48

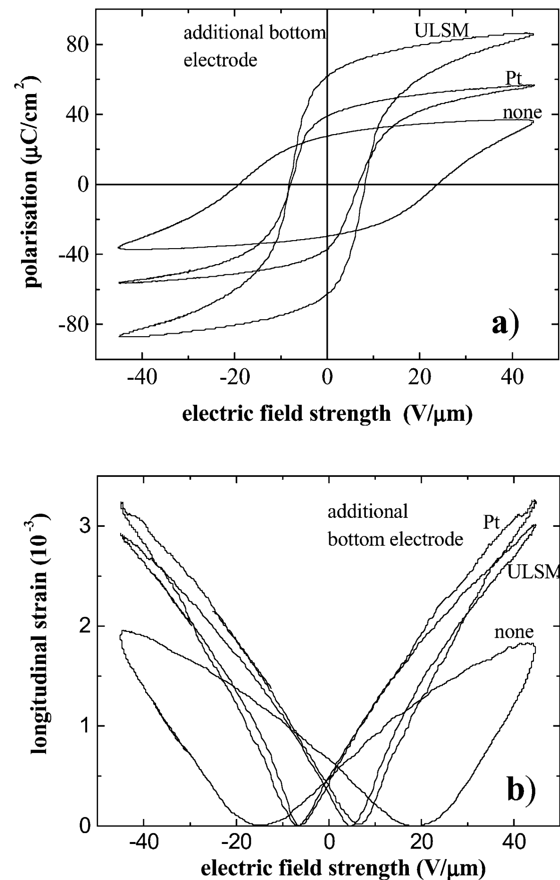

Fig. 8. Dielectric and electromechanical hysteresis loops for different types of substrate electrodes (film thickness 0.8 μm).

[1] Courtesy of Professor Dr. Rainer Waser, RWTH Aachen.

seems to be minimized, but is not suppressed completely.

3.2.2. Thickness dependence of PZT-films prepared on ULSM-electrodes

In order to investigate the influence of additional substrate electrodes in more detail, the thickness dependence of PZT films was investigated again. For that purpose, a series of samples with varying PZT film thicknesses was prepared on ULSM covered Hastelloy substrates. In Fig. 9, the thickness dependence of the dielectric permittivity and the piezoelectric coefficient d_{33} are plotted. For comparison, the data for films prepared directly on the metallic substrate are shown again.

As in the case of PZT films deposited directly on Hastelloy substrates, a linear dependence in the plot of $1/C_{film}$ versus t_{film} is found. The values obtained from the data fitting according to Eq. 1 are shown in Table 2. The dielectric permittivity ϵ_{33} of the pure film is nearly independent of the type of substrate electrode, whereas the capacitance of the interface layer for films on ULSM is about three times the value for films prepared directly on the Hastelloy substrate.

A similar behavior is found for the piezoelectric coefficient d_{33}. For the films on ULSM electrodes the values are higher and the thickness dependence is much less pronounced. Fitting the data according to Eq. 2, a piezoelectric coefficient of the pure PZT film of about 110 pm/V is obtained, which is only slightly higher than the values $d_{33,\mathrm{film}}$ obtained for PZT films on Hastelloy substrates without additional electrode (see Section 3.1.1).

Fig. 10 shows the dielectric and electromechanical hysteresis loops for films on ULSM electrodes. The dielectric hysteresis loops have a nearly rectangular shape. Typical values of remanent and maximum polarisation are 35 and 45 μC/cm^2, respectively, which are comparable with values found for films prepared directly on Hastelloy substrates. On the other hand, the coercive field strength is much smaller, and their thickness dependence is much weaker than for films prepared directly on the Hastelloy substrate. This can be seen from Fig. 11, which shows the coercive field strength for

Table 2
Characteristic properties of the interface layer and of the undisturbed PZT film for PZT films on unelectroded Hastelloy and on ULSM electrodes

PZT-films on	$C_{\mathrm{Interface}}$ (nF)	ε_{33} (ε_0)	$d_{33,\mathrm{film}}$ (pm/V)	$E_{\mathrm{C,film}}$ (V/μm)
pure Hastelloy	1.54	606	93	7.1
ULSM-electroded Hastelloy	5.15	529	110	4.7

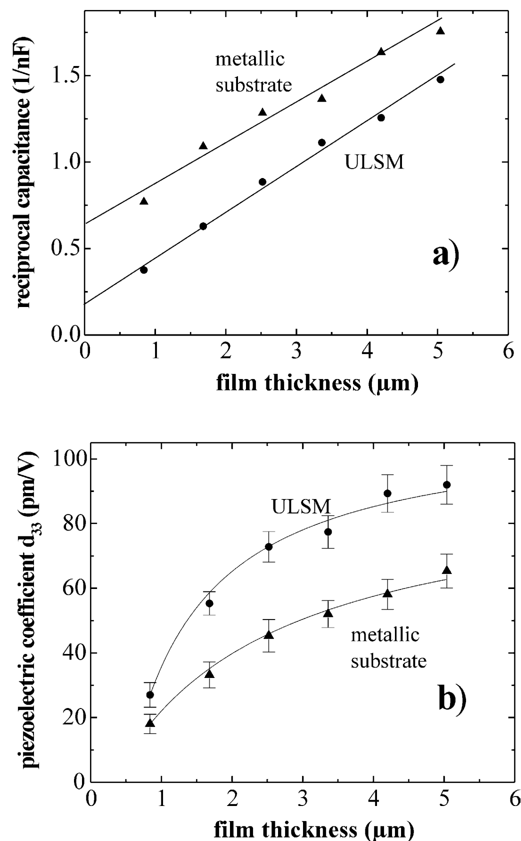

Fig. 9. Thickness dependence of the reciprocal capacitance and the piezoeletric coefficient d_{33} for films with and without ULSM electrode; the lines are fits to the model explained in the text.

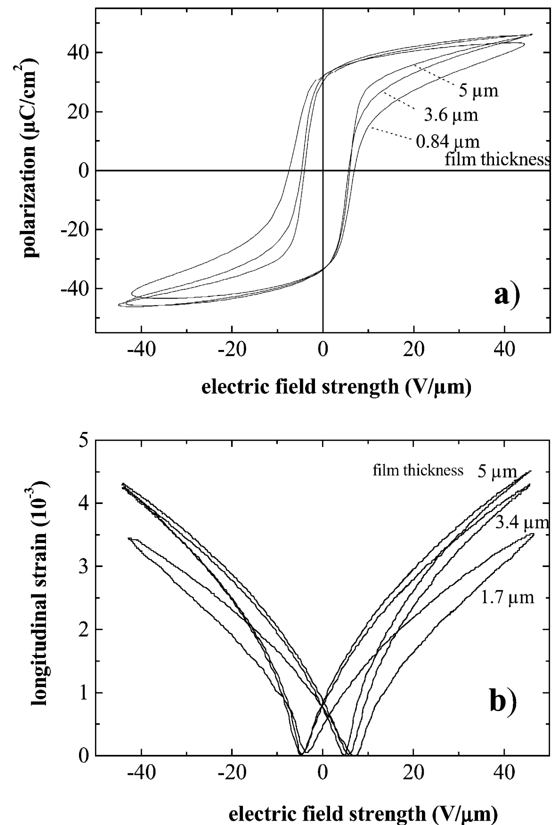

Fig. 10. Dielectric and electromechanical hysteresis loops for PZT-films on ULSM electrode with different film thicknesses.

films prepared on pure and ULSM-electroded Hastelloy as a function of film thickness, respectively.

Even the thinnest film on the ULSM electrodes has a lower coercive field strength than the thickest film prepared on Hastelloy; for the 5 μm thick films the coercive field strength on the pure Hastelloy substrate is about twice of that of the corresponding film on ULSM-electrode.

On the other hand, fitting the data according to Eq. 4 provides a coercive field strength of 4.7 V/μm for the pure PZT film on the ULSM electrode, which is about 60% of the coercive field strength of films on unelectroded Hastelloy ($E_c = 7.1$ V/μm).

To summarize, oxidic electrodes do not enhance the properties of the undisturbed PZT films significantly, but reduce remarkably the influence of the postulated disturbed interface region; therefore better dielectric and electromechanical properties for films on ULSM electrodes and a less pronounced thickness dependence were obtained. For a 5 μm thick film, the measured data are very similar to those calculated for the undisturbed films.

However, the still remaining thickness dependence of the films on ULSM-electroded substrates indicates that the formation of a disturbed interface layer is not completely suppressed. Here, it is only possible to speculate about the origin and nature of this layer. For example, elements other than those in the case of the metallic substrate electrode may diffuse into the film during preparation, or the thickness of the interface layer may be much smaller than in the case of films on metallic substrate electrodes. Furthermore, there could be an interface layer between film and the gold top electrode that could play a major role.

3.3. Variations of the stoichiometry

For PZT bulk ceramics, the extrema of small and large signal dielectric and electromechanical properties usually are found around the morphotropic phase boundary at a Zr/Ti-ratio of 53/47. In order to check the position of these extrema for our PZT films on Hastelloy substrates, series of films with Zr/Ti-ratios between 30/70 and 63/37 in the deposition solutions were prepared and the properties of the films were investigated. Fig. 12 shows the XRD diffractograms of samples with an average film thickness of approximately 2 μm.

Compared with bulk ceramics, the peaks of the diffractograms are broadened, which complicates quantitative analysis. However, for different peaks of PZT(30/70), e.g. for the (112) and (100) peak, a splitting can clearly be observed. This indicates the existence of the tetragonal phase for that composition. On the other hand, for compositions between PZT(58/42) to PZT(48/52) no splitting was found. The asymmetric peaks for PZT(38/62) indicate a coexistence of both phases. From these results it is concluded that in the PZT films the region of the coexistence of the rhombohedral and the tetragonal phase is much broader compared to bulk ceramics with a typical width of 2 mol% and is shifted towards more Ti-rich compositions.

Fig. 13 shows the dielectric constant ϵ_{33} and the piezoelectric coefficient d_{33} as a function of the Zr/Ti-ratio. For comparison, data for bulk-ceramics are plotted, too. Both, dielectric and piezoelectric coefficients show a maximum for a composition of PZT(48/52), i.e. the maxima are shifted towards more Ti-rich films compared with bulk-ceramics, too. However, the "sharpness" of the maximum is much less pronounced than for bulk ceramics.

The dependence of the coercive field strength E_C and the remanent polarization P_{rem} on the Zr/Ti-ratio also support the assumed shift and broadening of the morphotropic phase boundary (Fig. 14). The value of E_C is small for Zr-rich compositions (rhombohedral phase in bulk ceramics), however, the lowest value is obtained

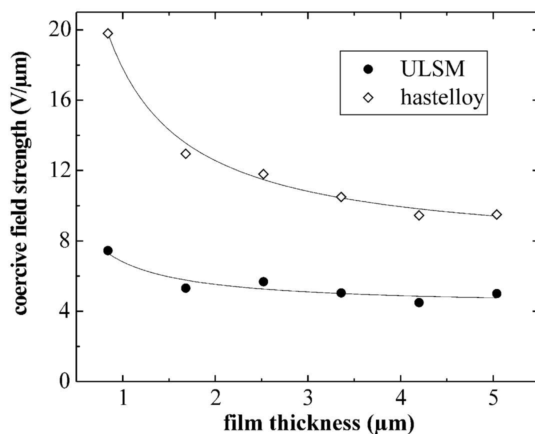

Fig. 11. Dependence of the coercive field strength on the film thickness from films with and without ULSM electrode; the lines correspond to a fit according to Eq. 4.

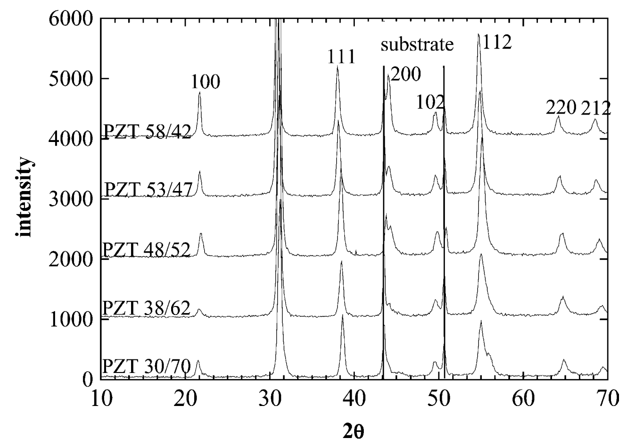

Fig. 12. XRD-diffractogramms of PZT-films with different Zr/Ti ratios; film thickness 2.2 μm.

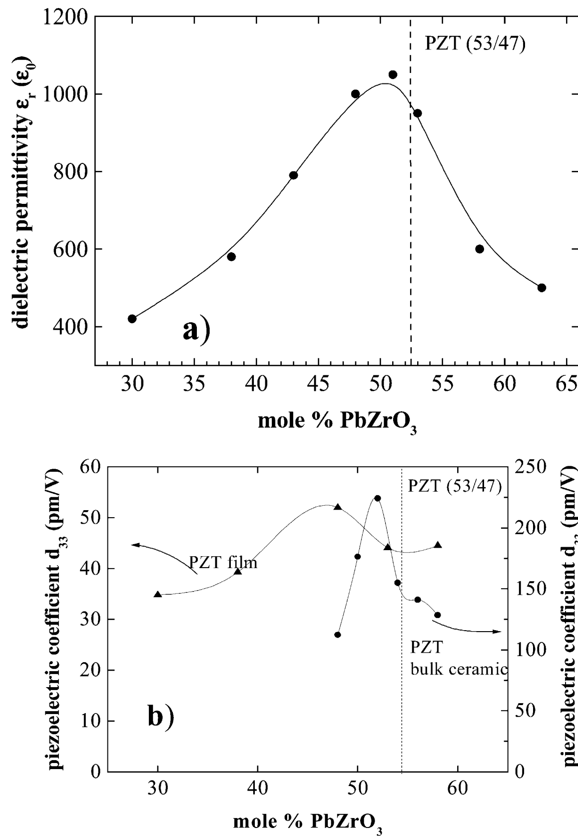

Fig. 13. Dielectric permittivity ε_{33} (a) and piezoelectric coefficient d_{33} (b) as a function of the Zr/Ti-ratio for PZT-films on Hastelloy substrate and bulk ceramics.

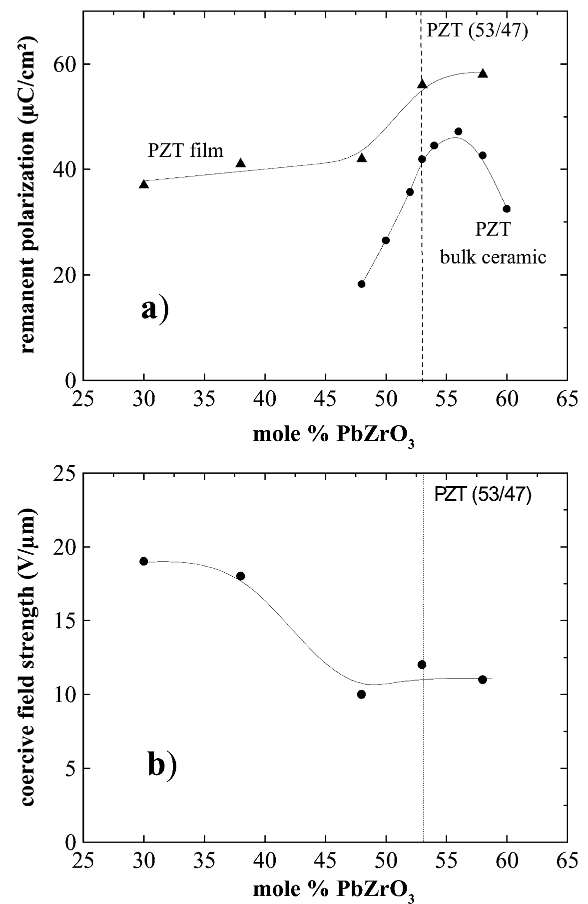

Fig. 14. Remanent polarization (a) and coercive field strength (b) as a function of the Zr/Ti-ratio for PZT-films on metallic substrate and bulk ceramics.

for PZT(48/52). At the same composition, the remanent polarization starts to drop, when going from Zr-rich to Zr-low compositions. For the Zr-low region, i.e. the tetragonal phase in bulk ceramics, higher coercive field strengths and lower remanent polarization values are observed for the films.

Summarizing, all observations point to a broadening of the morphotropic phase boundary and a shift towards more Zr-rich compositions in the films. The reasons are still under discussion. For example, it might be due to local fluctuations in the Zr/Ti ratio within the grains or the existence of secondary, Ti-enriched phases that cannot be detected by XRD. As a consequence, to achieve optimum di- and piezoelectric properties in the films the observed shift of the morphotropic phase boundary has to be compensated by adjusting the sol stoichiometry.

3.4. Application oriented investigations

3.4.1. Films with optimized piezoelectic properties

The results described in the previous chapters were used to produce films with optimized piezoelectric properties, i.e. piezoelectric charge coefficients and strains as high as possible. For that purpose PZT films consisting of 15 layers were deposited on ULSM-electroded Hastelloy substrates as described in Section 2.1. The resulting final thickness of the films, which were mechanically still stable and easy to handle, was about 6.4 μm. A nominal Zr/Ti ratio of 51/49 was chosen for the PZT, which is by 2 mol% shifted towards Zr-rich compositions compared to bulk ceramics.

Fig. 15 shows dielectric and electromechanical hysteresis loops. Both are narrow and well saturated. The dielectric hysteresis loop has a nearly rectangular shape and is characterized by a remanent polarisation of about 40 μC/cm^2, a saturation polarisation of about 50 μC/cm^2 and a coercive field strength of 5.2 V/μm. From the electromechanical hysteresis loop a maximum and a remanent strain of approximately 0.85 and 0.45% are observed, respectively.

Fig. 16 shows strain-field loops for unipolar voltages, which are of special interest for actuatoric applications. The loops are nearly hysteresis free. This indicates again the absence or at least a strong suppression of extrinsic contributions to the dielectric and electromechanical film properties. The strain of 0.28% at a maximum electric field strength of 40 V/μm corresponds to a

piezoelectric coefficient of 70 pm/V in the high signal behavior. In absolute units, this is an elongation of about 18 nm for a voltage of 260 V.

For standard poling and measuring conditions a piezoelectric coefficient $d_{33,\mathrm{meas}} = 96$ pm/V and a dielectric permittivity ϵ_{33} of about 620 were observed, which both indicate again that the films are well suited for sensoric applications.

3.4.2. Antiferroelectric PZT films with variations of the Zr/Ti ratio

PZT ceramics with a very low content of Ti are at room temperature in an antiferroelectric phase; they can be switched into a ferroelectric phase by applying an electric field and vice versa.[25] These transitions are accompanied by large strains, which make ceramics with these stoichiometries very attractive alternatives for electromechanical sensors and actuators.

In order to investigate if such phase switching films can be realized on metallic substrates too, PZT(98/2) films were prepared. In hysteresis loops for films prepared directly on the substrate, the phase-switching was found to be nearly absent. The characteristic dielectric double loop was only very weakly pronounced, and in the strain-field loops a switching was hardly visible, too (Fig. 17).

In contrast, as for the ferroelectric films, the situation changed drastically, when additional substrate electrodes were used. Fig. 18 shows dielectric and electromechanical hysteresis loops for a 2.2 μm thick PZT(98/2) film prepared on ULSM electrodes. Here, the double loop shape indicating the switching between antiferroelectric and ferroelectric state is well established. At low electric field strengths the films behave like a linear dielectric. At higher field strengths the switching into the ferroelectric state begins and saturation occurs at about 30–40 V/μm. From the loops taken at higher electric fields the critical field strength E_{C1} (Antiferroelectric→Ferroelectric transition) and E_{C2} (Ferroelectric→Antiferroelectric transition) were estimated to be about 20 V/μm and 10 V/μm, respectively. Also the shape of the strain-field loops clearly indicates a switching between antiferroelectric and ferroelectric state. For applied fields lower than E_{C1} the induced strain is less than 10^{-4}, whereas the phase switching is accompanied by a large elongation/contraction of the films. For a maximum field strength of 50 V/μm the "usable" strain is nearly 0.4%. This corresponds to an effective piezoelectric coefficient d_{33} of 80 pm/V. Moreover, when the electric field rises from 10 to 30 V/μm, a strain of about 0.25% is induced, which gives a differential effective piezoelectric coefficient of 125 pm/V.

The remanent strain of approximately 0.02% obtainable in Fig. 18 is not a true remanent strain, but rather a dynamic effect. After approximately 10 ms the remanent strain relaxes to zero. On one hand this shows that the phase switching in these films requires some time to proceed. On the other hand, the zero remanent strain indicates that the films completely return into the antiferroelectric state after removal of the electric field.

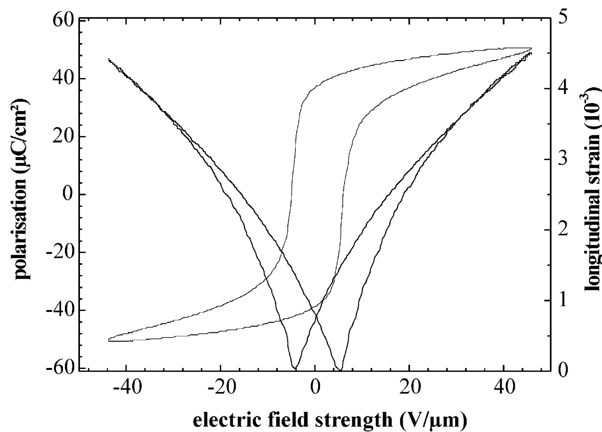

Fig. 15. Dielectric and electromechanical hysteresis loop of a film with optimized electromechanical properties.

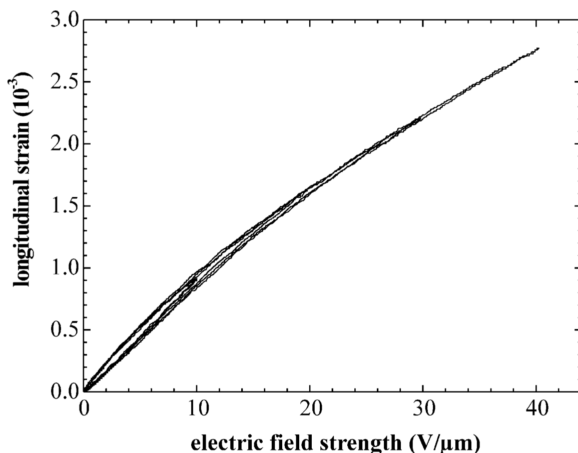

Fig. 16. Unipolar strain-field loops of a film with optimized piezoelectric properties for different exciting voltages.

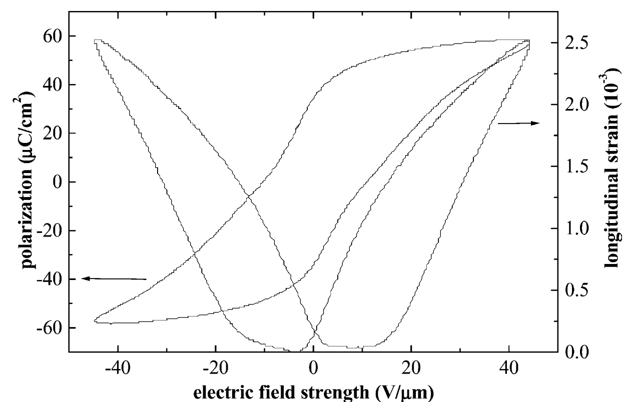

Fig. 17. Dielectric and electromechanical hysteresis loop for a PZT (98/2) film on Hastelloy substrates.

3.5. Investigations of the sensoric and actuatoric properties in the bending mode

In MEMS often the bending effect is used to realize the actuatoric and sensoric function. The bending effect, which is based on the transverse piezoelectric effect of the films, has some advantages compared with the usage of the longitudinal effects (d_{33}-mode). For example, the system substrate—PZT-film acts as a natural bimorph. Another reason is the much higher realizable deflection of cantilevers compared to a d_{33}-mode actuator. The PZT thin films on Hastelloy substrate were investigated for their suitability as sensoric or actuatoric bending elements.

3.5.1. Investigations of the non-resonance sensoric and actuatoric properties

Due to the easy integrability into metallic devices like housings, the use of the PZT films on Hastelloy substrates as sensor elements are very promising. For an investigation of the sensoric properties, a bending element 15×60 mm^2 in size was fixed at one end and a controlled macroscopic deflection of the bending element has been performed. From this deflection, the average local curvature of a defined sample area 10×10 mm^2 in size was calculated. The generated charge was determined by measuring the time dependent current and integrating it with respect to time. Typical correlations of the generated charge with the local transversal strain are shown in Fig. 19. As one can see, the generated charge scales linearly with the strain of the bending elements. Typical values for the generated charge are in the range of some 0.1 μC/cm^2. The generated charge is linear up to strains of more than 0.1%. Moreover, after mechanical cycling of the samples over a longer time, no significant decrease in the generated charge could be observed up to 10^4 cycles,[26,27] or in other words, this effect was stable for more than a year.

On the other hand, the substrate–film bimorph system can easily be used as a bending actuator. Fig. 20 shows the deflection at the end of 3.6 cm long actuator for different exciting voltages. For an applied electric field strength of 17 V/μm, the generated tip displacement is as high as 30 μm, which is in the range of 10^3 times more than the deflection in the d_{33}-mode. For example, such bending actuators may be used as a relay.

3.5.2. Investigation of resonance modes

Besides the linearity and the easy controllability of the piezoactive elements the knowledge of the mechanical resonance frequencies of the PZT film in the bimorph configuration is essential. Therefore, a frequency scan of the bending deflection of a sample (substrate thickness 200 μm) of 23×6 mm^2 in size was carried out. For excitation, only a small piezoelectric active area (4 μm thick PZT film), consisting of a circle 1 mm in diameter, was excited with an amplitude of 1.8 V/μm.

As one can see in Fig. 21, a typical resonance peak was found at the first resonance frequency of about 120 Hz with a small bandwidth of about 2.5 Hz. The maximum peak-peak deflection was about 30 μm at the first resonance frequency, which is in the range of one hundred times the deflection in nonresonance mode. Both facts illuminate that, due to the low mechanical

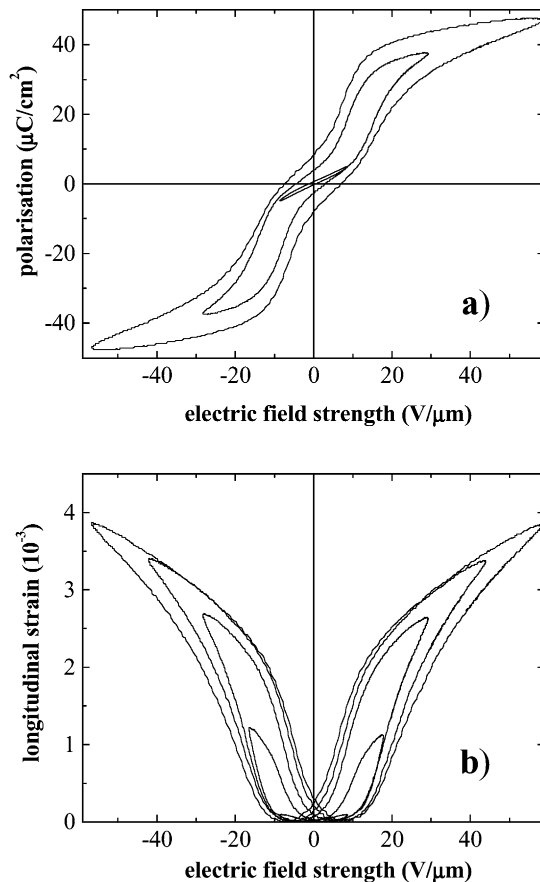

Fig. 18. Dielectric and electromechanical hysteresis loops of PZT (98/2) films on Hastelloy substrates with ULSM substrate electrodes.

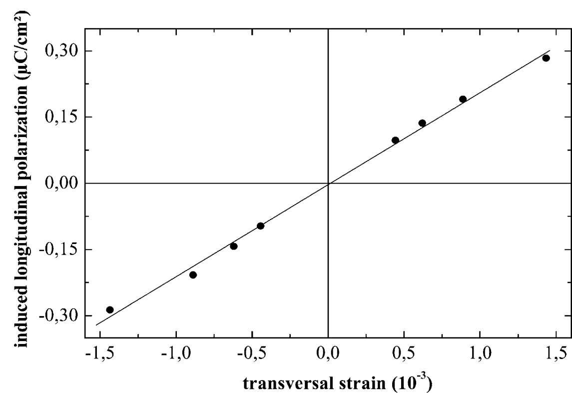

Fig. 19. Correlation of the charge generated by a quasistatic mechanical deflection of the bending element with the average local strain.

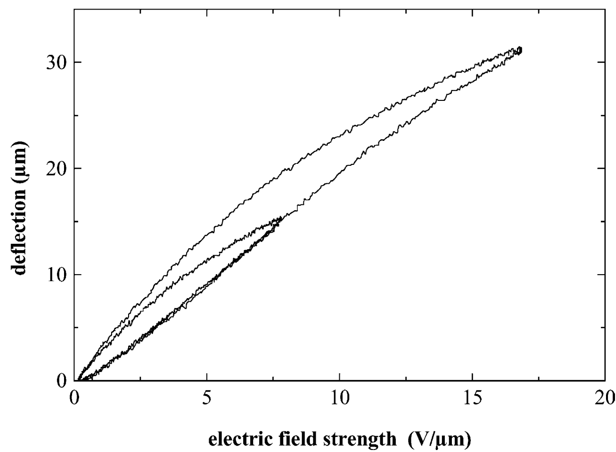

Fig. 20. Quasistatic deflection of the sample tip as a function of the applied field strength.

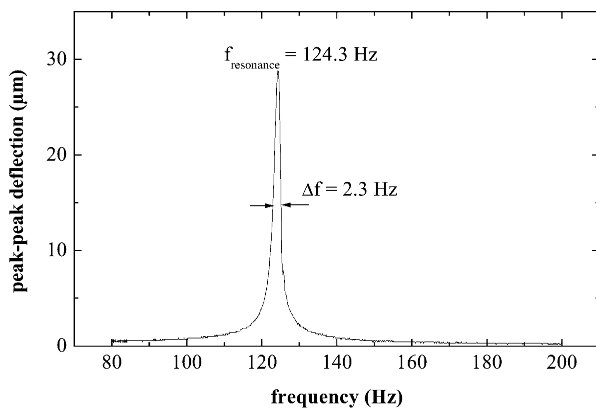

Fig. 21. Sample tip deflection as a function of frequency around the first mechanical resonance of a PZT thin film on metallic substrate (sample size: 23×6 mm^2, poled area: circle, 1 mm in diameter).

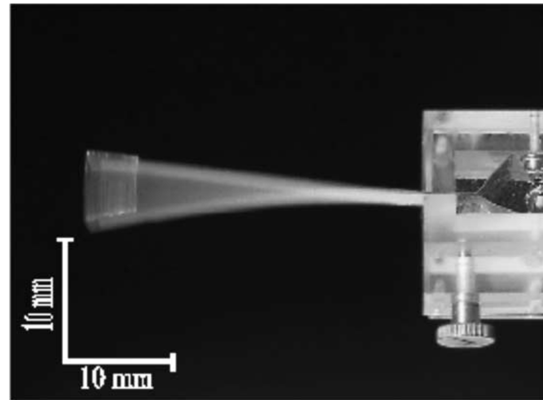

Fig. 22. Deflection of a piezoelectric cantilever with a length of 50 mm at the first mechanical resonance frequency at 37 Hz.

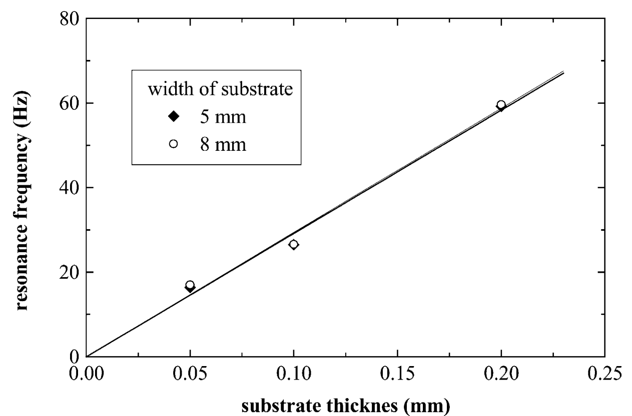

Fig. 23. First mechanical resonance frequency for different substrate thicknesses of the piezoelectric cantilever.

damping of the metallic substrate, a sharp resonance behavior can be observed.

For the dependence of the mechanical resonance frequencies on the bimorph dimensions larger piezoactive areas were used. Typical samples with areas 15×60 mm^2 in size were electroded and poled with a dc-field strength of 25 V/µm. The applied field strength was somewhat reduced during the investigations due to some defects within the large area of the sample. The applied excitation voltage for the mechanical resonance was always lower than 20 V absolute, corresponding to a maximum field strength of about 5–10 V/µm. With these parameters, the first mechanical resonance frequencies of the samples could be easily observed by the naked eye (see Fig. 22). Deflections of some hundred micrometers up to one mm were observed.

The mechanical resonance frequencies can be easily varied by changing the substrate length or thickness. As an expected result, the first resonance frequency is proportional to the substrate thickness (Fig. 23). On the other hand, the resonance frequency depends on the cantilever length as depicted in Fig. 24. The relations fit very well with the equations in the literature according to the sample geometry, where the resonance frequency is assumed to be proportional to the reciprocal square of the cantilever length.[28] Moreover, from both figures, one can see that the width of the cantilever has little influence on the resonance frequency.

4. Summary

It was shown that ferroelectric PZT films with thicknesses up to 6 µm can be deposited in good quality on metallic Hastelloy substrates by a sol-gel method. The observed strong thickness dependence of the properties was attributed to the formation of an interface layer between substrate and film.

The formation of this interface layer was minimized by supplying an additional bottom electrode between PZT film and substrate. No significant difference for the final film properties was observed between the usage of either metallic or oxidic electrodes. On one hand, both types led to a strong improvement of the overall

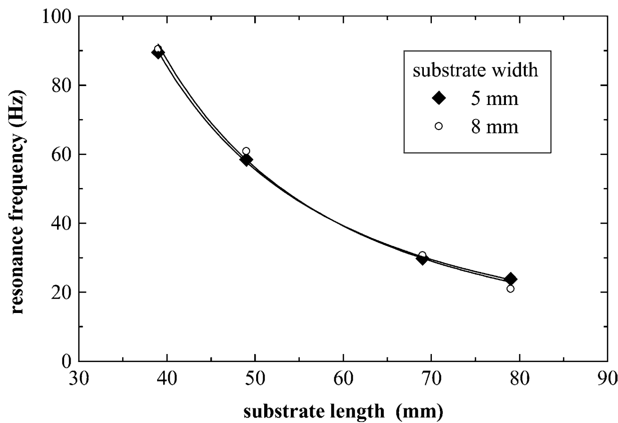

Fig. 24. First mechanical resonance frequency for different free lengths of the piezoelectric cantilever.

properties of the films and especially to a minimized thickness dependence of the film properties. On the other hand, the application of simple models showed that the properties of the pure, undisturbed PZT film are not influenced by the additional electrodes. Thus, the improvement of the overall film properties was explained by the suppression of the formation of the interface layer only.

Compared with bulk ceramics, the extrema of the film properties are shifted towards more Zr-rich stoichiometries, e.g. for a composition of PZT(48/52), a maximum of ϵ_{33} and d_{33} as well as a minimum of the coercive field strength was found. This correlates with XRD observations, which show a tetragonal splitting only for films with a Zr/Ti ratio lower than 48/52.

For realizing optimum piezoelectric properties, 6 μm thick PZT(51/49) films were deposited on ULSM electrodes by mutiple coating. These film showed nearly rectangular hysteresis loops with a coercive field strength as low as 5 V/μm; the piezoelectric coefficient d_{33} of these films was nearly 100 pm/V.

As an alternative, PZT(98/2) films with field induced phase transitions between AFE and FE phase could be deposited in a good quality on ULSM coated Hastelloy substrates, too. These films showed high strains and small hysteresis effects.

Finally, typical sensoric and actuatoric properties of the bimorphs consisting only of substrate–PZT-film were investigated. Measurements of the resonance frequency, the cantilever deflection and the generated charge by controlled bending a cantilever showed the suitability of the PZT-film–metallic substrate system for bending mode applications.

Acknowledgements

This work was supported by the Deutsche Forschungsgemeinschaft.

References

1. Uchino, K., *Piezoelectric Actuators and Ultrasonic Motors*. Kluwer Academic Publishers, London, 1997.
2. Cross, L. E., Ferroelectric materials for electromechanical transducer applications. *Jpn. J. Appl. Phys.*, 1995, **34**, 2525–2532.
3. Haun, M. J., Zhang, Z. Q., Furman, E., Jang, S. and Cross, L. E., Electrostrictive properties of the lead zirconate titanate solid-solution system. *J. Am. Ceram. Soc.*, 1989, **72**, 1140–1144.
4. Polla, D., Microelectromechanical systems based on ferroelectric thin films. *Microel. Engin.*, 1995, **29**, 51–58.
5. Muralt, P., Kholkin, A., Kholi, M., Maeder, T. and Setter, N., Characterization of PZT thin films for micromotors. *Microel. Engin.*, 1995, **29**, 67–70.
6. Yi, G., Sayer, M., Wu, Z., Jen, C. and Bussiere, J., Piezoelectric lead zirconate titanate coatings on metallic wires. *Electron. Lett.*, 1989, **25**, 907–908.
7. Kholkin, A. L., Calzada, M. L., Ramos, P., Mendiola, J. and Setter, N., Piezoelectric properties of Ca-modified $PbTiO_3$ thin films. *Appl. Phys. Lett.*, 1996, **69**, 3602–3604.
8. Yi, G., Wu, Z., Sayer, M., Jen, C. and Bussiere, J., Sol gel processed piezoelectric PZT thin films. *Ceram. Transac.*, 1990, **11**, 363–374.
9. Löbmann, P., Seifert, S., Merklein, S. and Sporn, D., Lead zirconate titanate films prepared from soluble powders. In *9th Intern. Workshop on Glasses, Ceramics, Hybrids and Nanocomposites from Gels*. Sheffield, Great Britain, 1997.
10. Sporn, D., Merklein, S., Grond, W., Seifert, S., Wahl, S. and Berger, A., Sol-gel processing of perovskite thin films. *Microel. Engin.*, 1995, **29**, 161–168.
11. Hasenkox, U., Mitze, C. and Waser, R., Metal propionate synthesis of Magnetoresistive La1$-x$(Ca,Sr)xMnO3 thin films. *J. Am. Ceram. Soc.*, 1997, **80**, 2709–2713.
12. Landolt-Börnstein, *Numerical Data and Functional Relationships in Science and Technology, Vol. 16*. Springer, New York, 1981.
13. Steinhausen, R., Hauke, T. Seifert, W. et al., Clamping of ferroelectric thin films on substrates: influence on the effective piezoelectric coefficient d_{33}. *Proc. 11th Int. Symp. Appl. Ferroel.*, 1999, 93–96.
14. Lefki, K. and Dormans, G. M. J., Measurement of piezoelectric coefficients of ferroelectric thin films. *J. Appl. Phys.*, 1994, **76**, 1764–1767.
15. Khachaturyan, K., Mechanical fatigue in thin films induced by piezoelectric strains as a cause of ferroelectric fatigue. *J. Appl. Phys.*, 1995, **77**, 6449–6455.
16. Yoo, I. K. and Desu, S. B., Modelling of the hysteresis of ferroelectric thin films. *Phil. Mag. B*, 1994, **69**, 461–469.
17. Larsen, P. K., Dormans, G. J. M., Taylor, D. J. and van Veldhoven, P. J., Ferroelectric properties and fatigue of $PbZr_{0.51}Ti_{0.49}O_3$ thin films of varying thickness: blocking layer model. *J. Appl. Phys.*, 1994, **76**, 2405–2413.
18. Miller, S. L., Nasby, R. D., Schwank, J. R., Rodgers, M. S. and Dressendorfer, P. V., Device modeling of ferroelectric capacitors. *J. Appl. Phys.*, 1990, **68**, 6463–6471.
19. Tagantsev, A. K., Landivar, M., Colla, E. and Setter, N., Identification of passive layers in ferroelectric thin films from their switching parameters. *J. Appl. Phys.*, 1995, **78**, 2623–2630.
20. Cho, S. J., Phase development of PZT Thin Films on Steel Substrates with Respect to Secondary Phases. Diploma thesis, University of Würzburg, Germany, 1997.
21. Takahashi, S., Effects of impurity pinning in lead zirconate–titanate ceramics. *Ferroelectrics*, 1982, **4**, 141.
22. Maeder, T., Muralt, P., Sagalowicz, L., Reaney, I. and Kohli, M. et al., $Pb(Zr,Ti)O_3$ thin films on zirconium membranes for micromechanical applications. *Appl. Phys. Lett.*, 1996, **68**, 776–778.

23. Vijay, D. P. and Desu, S. B., Electrodes for PbZrxTi1−xO3(PZT) ferroelectric thin films. *J. Electrochem. Soc.*, 1993, **140**, 2640.
24. van der Pauw, L. J., A method of messuring specific resistivity and Hall effect of discs of arbitrary shape. *Philips Res. Reports*, 1958, **13**, 1–9.
25. Brooks, K. G., Udayakumar, K. R., Chen, J., Selvaraj, U. and Cross, L. E., Smart ferroelectric films and fibers; applications in micromechanics. *Mat. Res. Soc. Symp. Proc.*, 1992, **276**, 11–23.
26. Giersbach, M., Seifert, S., Sporn, D., Hauke, T. and Beige, H., Piezoelectric proper-ties of PZT thin films on metallic substrates. *Ferroelectrics*, 2000, **241**, 175–182.
27. Hauke, T., Beige, H., Giersbach, M., Seifert, S. and Sporn, D., Mechanical and electrical fatigue of PZT(53/47) films on metallic substrates. *Int. Ferroel.*, 2001, **35**, 219–228.
28. Gardeniers, J., Verholen, A., Tas, N. and Elwenspoek, M., Direct measurement of piezoelectric properties of sol-gel PZT films. *J. Kor. Phys. Soc.*, 1998, **32**, 1573–1577.